
Proceedings of the XXXIV International School of Semiconducting Compounds, Jaszowiec 2005

Pb_{1-x}Mn_xTe Crystals as a New Thermoelectric Material

V. OSINNIY, A. JĘDRZEJCZAK, W. DOMUCHOWSKI, K. DYBKO,
B. WITKOWSKA AND T. STORY

Institute of Physics, Polish Academy of Sciences
al. Lotników 32/46, 02-668 Warsaw, Poland

We studied experimentally thermoelectric properties of *p*-type bulk crystals of Pb_{1-x}Mn_xTe and Pb_{1-x-y}Ag_yMn_xTe ($0 \leq x \leq 0.083$ and $y \leq 0.017$) at room and liquid nitrogen temperatures. Model calculations of the thermoelectric figure of merit parameter (Z) involved the analysis of carrier concentration, carrier mobility, density of states as well as electronic and lattice contributions to the thermal conductivity of PbMnTe. In the analysis we took into account the main effect of Mn concentration on the band structure parameters of PbMnTe, i.e. the increase of the energy gap. The analysis of electrical, thermoelectric, and thermal properties of Pb_{1-x}Mn_xTe crystals showed that, at room temperature, the maximum values of the parameter Z occur in crystals with Mn content $0.05 \leq x \leq 0.07$ and are comparable with a maximal value of Z observed in PbTe. At $T = 400$ K the increase in the parameter Z by 10% is expected in Pb_{1-x}Mn_xTe crystal (as compared to PbTe) for a very high concentration of holes of about $p = 5 \times 10^{19} \text{ cm}^{-3}$. The experimental data correctly reproduce the theoretical $Z(p)$ dependence.

PACS numbers: 72.20.Pa, 72.80.Jc

1. Introduction

The search for new solid state materials for coolers and power generators based on thermoelectric Peltier and Seebeck effects remains one of the key issues in materials science. The efficiency of these devices at a temperature T is determined by the thermoelectric figure of merit parameter $ZT = \alpha^2\sigma/\kappa$, where α is the Seebeck coefficient, σ is the electrical conductivity, and κ is the thermal conductivity. For a broad commercial application of these materials the figure of merit parameter should be greater than unity ($ZT \geq 1$). Two main directions of research in the field of thermoelectricity are connected with low dimensional structures based on

the well-known thermoelectric materials (such as PbTe and Bi₂Te₃ based alloys) or materials with anomalous electrical or thermal properties (e.g., skutterudites, half-Heusler intermetallic compounds) [1]. The first case is mainly connected with quantum size effects modifying the electron density of states at the Fermi level. In the second case, new bulk materials having anisotropic thermoelectric properties and reduced lattice thermal conductivity are studied. These are usually materials with a high atomic mass and/or alloys with three and more very different elements (e.g., the so-called “phonon rattlers”) [1]. The general concept of the good thermoelectric material is summarized as “phonon-glass electron-crystal” which means that the material should have a low thermal conductivity as in a glass and a high electrical conductivity as in a crystal [2]. Some magnetic ions are expected to improve the figure of merit parameter due to the resonant scattering of phonons by these ions leading to a stronger decrease in thermal conductivity as compared to a drop of the electrical conductivity due to their presence (e.g., in PbTe:Fe [3]). The aim of this research is to find materials with thermoelectric performance at a room temperature better than in Bi₂Te₃ based alloys. The optimum operating temperatures T_{opt} of the thermoelectric devices based on the different thermoelectric materials cover a broad range: for Bi₂Te₃ group it is $T_{\text{opt}} \approx 300$ K, for PbTe group, $T_{\text{opt}} \approx 800$ K and for Si-Ge group, $T_{\text{opt}} \approx 1500$ K [4].

In this work we investigated the thermoelectric properties of p -type bulk crystals of PbMnTe and PbAgMnTe. The main idea of this research is based on the observation that the change of the band structure of PbMnTe with an increasing Mn content is similar to the evolution of the band structure of PbTe with the temperature increase. The use of PbMnTe crystals may result in a decrease in the optimum operating temperature of the thermoelectric device. The energy gap of PbMnTe increases with an increasing temperature as well as with an increasing Mn concentration x according to the formula: $E_g = |171.5 + \sqrt{(12.8)^2 + 0.19(T + 20)^2}| + 2500x$ [meV]. Therefore one can obtain

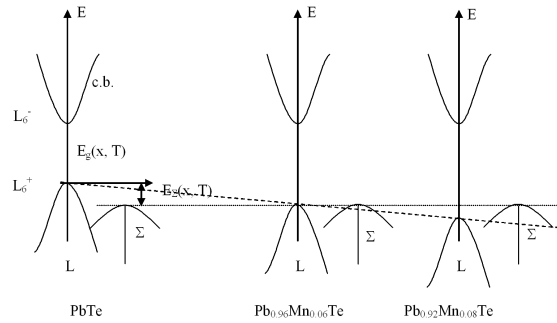


Fig. 1. A model of band structure evolution in $\text{Pb}_{1-x}\text{Mn}_x\text{Te}$ at room temperature with increasing Mn ions content. In PbTe the top of the band of heavy holes (Σ) is located below the top of the band of light holes (L_6^+). In the $\text{Pb}_{1-x}\text{Mn}_x\text{Te}$ crystals with Mn content $x \geq 0.06$ the Σ -band is expected to form the top of the valence band.

in Pb_{1-x}Mn_xTe at $T = 300$ K the band structure parameters similar to the parameters of the host PbTe material at $T = 800$ K. As shown in Fig. 1 the energy gap $L_6^+ - L_6^- (E_g)$ increases with the increase in Mn content whereas the energy interval $L_6^- - \Sigma$ between the bottom of the conduction band and the top of the Σ -band of heavy holes does not change. For the materials with the Mn content above 6 at.% the top of the valence band of heavy holes is located above the band of light holes which leads to the increase of the contribution of heavy holes to the thermoelectric effects.

2. Crystal characterisation and thermoelectric measurements

The bulk crystals of Pb_{1-x}Mn_xTe and Pb_{1-x-y}Ag_yMn_xTe ($0 \leq x \leq 0.083$ and $y \leq 0.017$) were grown by the vertical Bridgman method in quartz ampoules with their inner wall covered with graphite. The ampoule with the proper amount of polycrystalline PbTe, Mn, Ag, and Te was heated up to 970°C and removed from the furnace with the speed of about 2 cm/day.

The chemical composition of the samples was checked by energy dispersive X-ray fluorescence analysis which revealed a good chemical homogeneity of the alloys. The X-ray diffraction measurements showed that the crystals possessed the rock-salt crystal structure with the lattice parameter decreasing with the increasing Mn content according to the Vegard law.

In order to change the carrier concentration an isothermal annealing in Te vapour was performed on a series of samples with different Mn content. The concentration range obtained in this way was $p = (1 - 6) \times 10^{18} \text{ cm}^{-3}$ for PbMnTe crystals. To increase further the hole concentration in PbMnTe crystals one can heavily dope, e.g. with Ta, Na or Ag. In our work we grew bulk PbAgMnTe crystals (under the same growth conditions as described above) with silver concentration up to 1.7 at.%. The process of isothermal annealing of those crystals resulted in a change of the hole concentration between $p = 1 \times 10^{19} \text{ cm}^{-3}$ and $p = 6 \times 10^{19} \text{ cm}^{-3}$. Here we would like to remark that not all the elements which increase the hole concentration in PbMnTe can be used in our case. For example, the incorporation of Sn in PbMnTe does increase the hole concentration but simultaneously it narrows the energy gap E_g .

To experimentally characterize the thermoelectric properties of PbMnTe and PbAgMnTe, the measurements of electrical conductivity, Hall effect, Seebeck effect, and Peltier effect were carried out at room and liquid nitrogen temperatures. The main goal of these experiments was to determine the dependence of the thermoelectric figure of merit parameter ZT of PbMnTe and PbAgMnTe on both the carrier concentration and the Mn content. The measurements of the thermoelectric power (Seebeck coefficient) were carried out using a standard method with the temperature gradient along the sample $\Delta T = 3-6$ K. The temperature difference in the sample was monitored by fine Cu-constantan thermocouples mounted to the sample in thin drilled holes using conducting silver paste. The typical size of the

samples was $10 \times 3 \times 3 \text{ mm}^3$. The Mn concentration dependence of thermoelectric power in the PbMnTe crystals with $p \approx 2 \times 10^{18} \text{ cm}^{-3}$ is presented in Fig. 2 (open squares). Very high values of thermoelectric power were found for PbMnTe samples with $x > 0.06$ indicating that the figure of merit parameter of PbMnTe can be improved in comparison to that in PbTe.

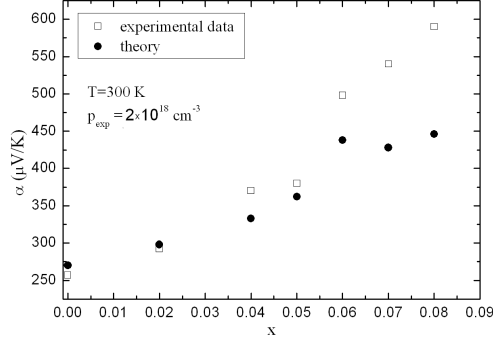


Fig. 2. Mn content dependence of thermoelectric power in p -PbMnTe at room temperature for crystals with practically the same carrier concentration $p \approx 2 \times 10^{18} \text{ cm}^{-3}$.

Peltier effect measurements were carried out on the same samples on which the thermoelectric power was measured. In order to determine the thermoelectric figure of merit parameter by the Harman method [5] one needs to compare DC and AC resistivities according to formula $ZT = (R_{DC} - R_{AC})/R_{AC}$. The DC resistivity was measured by the standard four-probe method and the AC resistivity measurements were performed using AVS-47 resistance bridge. The voltage leads were mounted in thin drilled holes and the current leads were glued on the sides of samples. To avoid Joule heating at the current contacts we additionally deposited chemically gold contact pads.

The carrier concentration and carrier mobility were determined from the electrical conductivity and Hall effect measurements carried out by the standard DC four-probe method. The good ohmic electrical contacts were provided by soldering of indium to golden contact pads deposited on the sample surface.

3. Theoretical calculations and discussion

In our model theoretical analysis we took into account the fact that with an increasing Mn concentration the energy gap $E_g = E_{L_6^-} - E_{L_6^+}$ in $\text{Pb}_{1-x}\text{Mn}_x\text{Te}$ increases whereas the energy separation between the top of the band of light holes and the band of heavy holes (E_{Σ}) decreases (see Fig. 1). The valence band of light holes is non-parabolic with the energy dispersion relation described by the Kane model: $E(1 + E/E_g) = \hbar^2(k_t^2/m_t^* + k_l^2/m_l^*)$, where \hbar is the Planck constant, $k_{t,l}$ are the components of the wave vector and $m_{t,l}^*$ are the components of the effective mass tensor (symbols t and l correspond to the transverse and longitudinal

components, respectively, referring to the long axis of the Fermi ellipsoid along [111] direction). The valence band of the heavy holes is described by a parabolic $E(k)$ relation with the effective mass (density-of-states mass) $m_{d\Sigma} = 1.2m_0$ [6]. The main carrier scattering mechanisms at room temperature are: the scattering by acoustic phonons (scattering parameter $r = 0$), the scattering by optical phonons ($r = 3/2$), and the scattering by neutral ions ($r = 1/2$). In order to consider the influence of all scattering mechanisms we calculated the reduced scattering parameter $r^* = \sum(r_i/\mu_i) / \sum(1/\mu_i)$ [7], where r_i and μ_i are the scattering parameters and the carrier mobilities which are due to each separate scattering process. In the Kane model, the effective mass of light holes can be described by $m^* = m_0^*(1 + 2E/E_g)$, where m_0^* is the mass at the top of the band of light holes. For each Mn concentration, we took into account the contributions of both valence bands to the electrical, thermoelectric, and thermal properties. The lattice thermal conductivity was taken as $\lambda_l = 2$ W/mK for all Mn contents. It agrees with the experimental data presented in [8, 9] where thermal conductivity of the same materials was studied. By changing the Fermi level position in PbMnTe we studied the carrier concentration dependence of the carrier mobility, the Hall constant, the thermoelectric power, the thermoelectric power factor, electronic contribution to thermal conductivity, and the figure of merit parameter ZT .

In Fig. 3 the dependence of the carrier mobility on Mn concentration is shown for PbMnTe crystals with the same hole concentration. In our calculations we adopted the band structure and the scattering parameters which were used to describe the electrical properties of the best bulk PbTe monocrystals [7]. The theoretical values turned out to be higher than the experimental ones for all Mn concentrations studied. It is, most likely, related to the fact that our PbMnTe crystals are polycrystals and consist of the great amount of small grains. Due to the scattering by the grain boundaries the electrical quality of our crystals is worse than one of the best PbMnTe monocrystals. Possibly, one should include

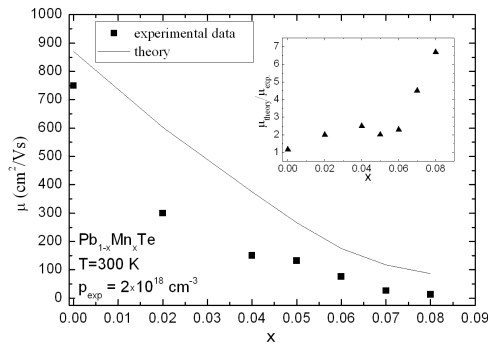


Fig. 3. Comparison of theoretical and experimental carrier mobility in p -PbMnTe with different Mn concentration. Inset shows that the biggest deviation of the experimental data from the theoretical calculations is for samples with Mn content above 6 at.%.

in the consideration an additional scattering mechanism by ionized impurities. Absolute values of the carrier mobility in PbMnTe crystals with Mn concentration above 5 at.% are very low both at the room and the liquid nitrogen temperatures. Isothermal annealing of the crystals improves the electrical quality of PbMnTe with Mn content up to 5 at.%. Unfortunately, the electrical properties of the annealed samples with higher Mn content did not show any essential improvement. We suspect that a part of Mn ions may occupy interstitial lattice positions. These Mn ions are donors which compensate free holes and form charged scattering centres.

In Fig. 2 one can notice that good agreement between theoretical and experimental data on thermoelectric power in $\text{Pb}_{1-x}\text{Mn}_x\text{Te}$ is observed only for crystals with Mn $x \leq 0.05$. For higher Mn concentrations, the theoretical values are considerably lower than the experimental ones. Even if we additionally include in our analysis the scattering mechanism by ionized impurities ($r = 2$) we cannot reproduce the high values of the thermoelectric power. Such enhancement of thermoelectric power can be connected with an increase in the effective mass of heavy holes with increasing Mn content. The attempt to determine the Mn concentration dependence of the effective mass of the density of states of heavy holes was undertaken in [10].

The theoretical analysis of the electronic part of the thermal conductivity showed that the contribution due to the holes becomes essential only for the carrier concentration above $p = 1 \times 10^{19} \text{ cm}^{-3}$ in PbTe. For the samples with Mn, this value rises.

Based on the carrier concentration dependence of the thermoelectric power, thermal conductivity, and electrical conductivity we can determine the carrier concentration for which the figure of merit parameter is at maximum in PbMnTe crystals. It was found that this carrier concentration increases with increas-

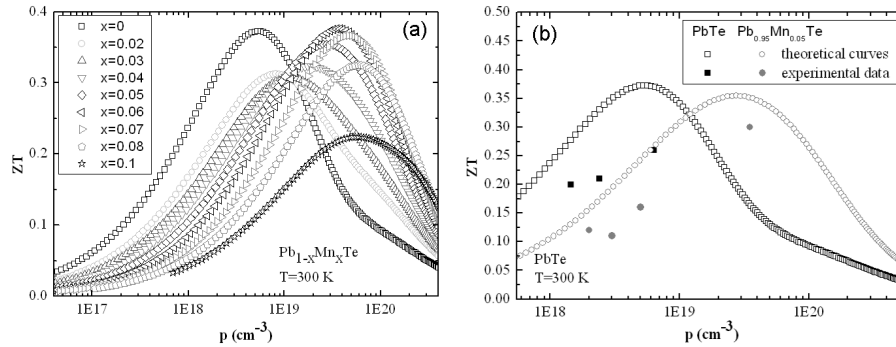


Fig. 4. Thermoelectric figure of merit parameter ZT in PbMnTe at room temperature. (a) theoretical calculations of the parameter ZT in $\text{Pb}_{1-x}\text{Mn}_x\text{Te}$ ($x < 0.1$) as a function of Mn content, (b) thermoelectric figure of merit parameter in bulk PbTe and $\text{Pb}_{0.95}\text{Mn}_{0.05}\text{Te}$ crystals: open symbols present theoretical calculations whereas solid symbols show the experimental data.

ing Mn content, with the maximum value of ZT being lower than in PbTe for $0.01 < x < 0.04$, similar to the maximum in PbTe for $0.05 \leq x \leq 0.07$ and much smaller for $x > 0.07$ (Fig. 4a). This non-monotonic behaviour is connected with the participation of two types of holes in the electron transport. In the first region ($0 \leq x \leq 0.05$), the light holes are responsible for the maximum of ZT , whereas in the second region ($x \geq 0.06$) the heavy holes play a key role in electron transport. Isothermal annealing results in the increase in the electrical conductivity and the decrease in thermoelectric power (due to increasing carrier concentration). As a result, the figure of merit parameter increases about twice for most samples with different Mn content. The experimental data describe correctly the theoretical tendency in PbTe and in $\text{Pb}_{0.95}\text{Mn}_{0.05}\text{Te}$ crystals but the absolute values of the calculated parameter ZT are smaller by about 10–15% (Fig. 4b).

The theoretical analysis of the thermoelectric parameters in PbMnTe also applies to higher temperatures. Our model analysis predicts that at $T = 400$ K $\text{Pb}_{1-x}\text{Mn}_x\text{Te}$ crystals with $0.05 \leq x \leq 0.07$ can be competitive thermoelectric materials to PbTe with figure of merit parameter about 10% higher than in PbTe.

4. Summary

We examined experimentally and theoretically the thermoelectric properties of PbMnTe. The thermoelectric power, electrical conductivity, carrier concentration, and the figure of merit parameter measurements were carried out for the bulk $\text{Pb}_{1-x}\text{Mn}_x\text{Te}$ and $\text{Pb}_{1-x-y}\text{Ag}_y\text{Mn}_x\text{Te}$ crystals ($0 \leq x \leq 0.083$; $y \leq 0.017$). The strong increase in thermoelectric power was found in $\text{Pb}_{1-x}\text{Mn}_x\text{Te}$ crystals as compared to PbTe crystals. We considered the model description of the Mn ions influence on the transport and thermoelectric parameters in PbMnTe crystals. It takes into account the temperature and Mn content dependence of energy gap $E_g(x, T)$ and the separation energy between the band of light holes and the band of heavy holes $E_\Sigma(x, T)$. The theoretical analysis of the influence of Mn concentration on the figure of merit parameter ZT in $\text{Pb}_{1-x}\text{Mn}_x\text{Te}$ showed that the crystals with $0.05 \leq x \leq 0.07$ can have the thermoelectric parameters better than PbTe crystals. The critical point in the optimization of these parameters is the growth of the PbMnTe crystals, especially for the Mn concentration above 5 at.%.

Acknowledgments

Work supported by the State Committee for Scientific Research project PBZ/KBN/044/P03/2001.

References

- [1] G. Chen, M.S. Dresselhaus, G. Dresselhaus, J.-P. Fleurial, T. Caillat, *Int. Mater. Rev.* **48**, 45 (2003).
- [2] G. Slack, in: *CRC Handbook of Thermoelectrics*, Ed. D.M. Rowe, CRC Press, Boca Raton 1995, p. 407.
- [3] D.T. Morelli, J.P. Heremans, C.M. Thrush, *Phys. Rev. B* **67**, 35206 (2003).
- [4] C. Wood, *Reports on Progress in Physics* **51**, 4 (1988).
- [5] T.C. Harman, *J. Appl. Phys.* **29**, 1201 (1957).
- [6] G.V. Lashkarev, M.V. Radchenko, F.F. Sizov, E.I. Slynko, V.V. Tetyorkin, *Ukrainskii Fizicheskii Zhurnal* **26**, 7 (1981).
- [7] W. Zawadzki, *Adv. Phys.* **23**, 435 (1974).
- [8] E.I. Rogachova, *Jpn. J. Appl. Phys.* **32S**, 3 (1993).
- [9] E.I. Rogachova, I.M. Krivulkin, *Fiz. Tverd. Tela* **43**, 1000 (2001).
- [10] P. Łazarczyk, M.V. Radchenko, G.V. Lashkarev, T. Story, K. Dybko, R.R. Gałązka, *Semicond. Sci. Tech.* **13**, 989 (1998).